A *Drosophila melanogaster* model of spinal muscular atrophy reveals a function for SMN in striated muscle

T.K. Rajendra, Graydon B. Gonsalvez, Michael P. Walker, Karl B. Shpargel, Helen K. Salz, and A. Gregory Matera

Department of Genetics, Case Western Reserve University School of Medicine, Cleveland, OH 44106

Mutations in human *survival motor neurons 1* (*SMN1*) cause spinal muscular atrophy (SMA) and are associated with defects in assembly of small nuclear ribonucleoproteins (snRNPs) in vitro. However, the etiological link between snRNPs and SMA is unclear. We have developed a *Drosophila melanogaster* system to model SMA in vivo. Larval-lethal *Smn*-null mutations show no detectable snRNP reduction, making it unlikely that these animals die from global snRNP deprivation. Hypomorphic mutations in *Smn* reduce dSMN protein levels in the adult thorax, causing flightlessness and acute muscular atrophy. Mutant flight muscle motoneurons display pronounced axon routing and arborization defects. Moreover, *Smn* mutant myofibers fail to form thin filaments and phenocopy null mutations in *Act88F*, which is the flight muscle–specific actin isoform. In wild-type muscles, dSMN colocalizes with sarcomeric actin and forms a complex with α-actinin, the thin filament crosslinker. The sarcomeric localization of Smn is conserved in mouse myofibrils. These observations suggest a muscle-specific function for SMN and underline the importance of this tissue in modulating SMA severity.

Introduction

Spinal muscular atrophy (SMA) is a genetic disorder associated with recessive loss-of-function mutations in the human *survival motor neurons 1* (*SMN1*) gene (Lefebvre et al., 1995). SMA is a broad-spectrum disorder whose severity is inversely proportional to levels of full-length SMN protein (Nicole et al., 2002). The most severe form of SMA is also the most common one, and these patients typically die within the first 2 yr of life (Ogino and Wilson, 2004). SMA is characterized by loss of motoneurons from the anterior horn of the spinal cord and progressive muscular atrophy in the limbs and trunk, usually culminating in respiratory failure (Ogino and Wilson, 2004).

SMN is the central member of a large oligomeric protein complex implicated in a variety of subcellular processes, including pre-mRNA transcription and splicing, RNP biogenesis and transport, neuritogenesis, and axonal pathfinding, as well as in the formation and function of neuromuscular junctions (Briese et al., 2005; Eggert et al., 2006). However, the only SMN function that has been well-documented to date is its role in the biogenesis of Sm-class small nuclear RNPs (snRNPs; Fischer et al., 1997; Meister et al., 2001; Pellizzoni et al., 2002). Despite the observation that SMA patient-derived *SMN1* mutations lead to defects in Sm-core assembly in vitro (Shpargel and Matera, 2005; Wan et al., 2005; Winkler et al., 2005), a definitive link between snRNP biogenesis and the etiology of the disease has not been established in a model organism.

Null mutations in single-copy *SMN* genes are lethal in every organism studied to date (Monani, 2005). In humans and higher primates, there are two *SMN* genes, *SMN1* and *SMN2* (Courseaux et al., 2003). *SMN2* is dispensable, but can partially compensate for homozygous loss of *SMN1* (Monani, 2005). Patients with additional copies of *SMN2* display milder phenotypes, a finding that has been confirmed using several transgenic mouse models (Monani, 2005). Because SMA is caused by reduced expression of SMN, modeling SMA in other genetically tractable organisms has been hampered by the need to create hypomorphic mutations. We describe the generation of a *Drosophila melanogaster* model of SMA. Hypomorphic *Smn* mutants are characterized by an inability to fly or jump, and they display severe neuromuscular defects. The analysis of this phenotype has led to the surprising discovery that SMN is a sarcomeric protein, implicating a muscle-specific function.

Correspondence to Greg Matera: a.matera@case.edu

Abbreviations used in this paper: DLM, dorsal longitudinal muscle; dsRNA, double-stranded RNA; DVM, dorsoventral muscle; IFM, indirect flight muscle; MSM, male-specific muscle; SMA, spinal muscular atrophy; *SMN*, *survival motor neurons;* snRNP, small nuclear RNP.

The online version of this article contains supplemental material.

The Journal of Cell Biology, Vol. 176, No. 6, March 12, 2007 831–841
http://www.jcb.org/cgi/doi/10.1083/jcb.200610053

Results

D. melanogaster Smn functions in snRNP assembly

Smn (CG16725) is a single-exon gene in *D. melanogaster* (Fig. 1 A), encoding a 226-aa protein (Miguel-Aliaga et al., 2000). The expression profile shows that dSMN is highly expressed during embryogenesis, but that the levels decrease sharply during subsequent developmental stages (Fig. 1 B and not depicted). Because SMN is essential for Sm-core RNP assembly in human cells (Shpargel and Matera, 2005; Wan et al., 2005; Winkler et al., 2005), we investigated whether the *D. melanogaster* protein has a similar conserved function. Schneider 2 (S2) cells treated with double-stranded RNA (dsRNA) targeting *Smn*, but not *LacZ*, were efficiently and specifically depleted of dSMN (Fig. 1 C). As assayed by two independent methods, *Smn* dsRNA-treated S2 cells were deficient in assembly of new Sm cores (Figs. 1, D and E). Thus, we conclude that SMN's function in snRNP assembly is conserved in invertebrates.

Characterization of *Smn*-null mutants

A previous study identified two missense mutations (Smn^A and Smn^B; Fig. 1 A) in the conserved Y-G box of the *D. melanogaster* gene, the homozygous inheritance of which results in late-larval lethality (Chan et al., 2003). To identify additional alleles, we searched transposon insertion databases and found one *P* element and two piggyBac transposon insertions in both coding and noncoding regions of *Smn* (Fig. 1 A). EY14384 (henceforth referred to as Smn^E) is a *P* insertion located 94 bp upstream of the putative transcription start site, whereas f05960 (Smn^C) and

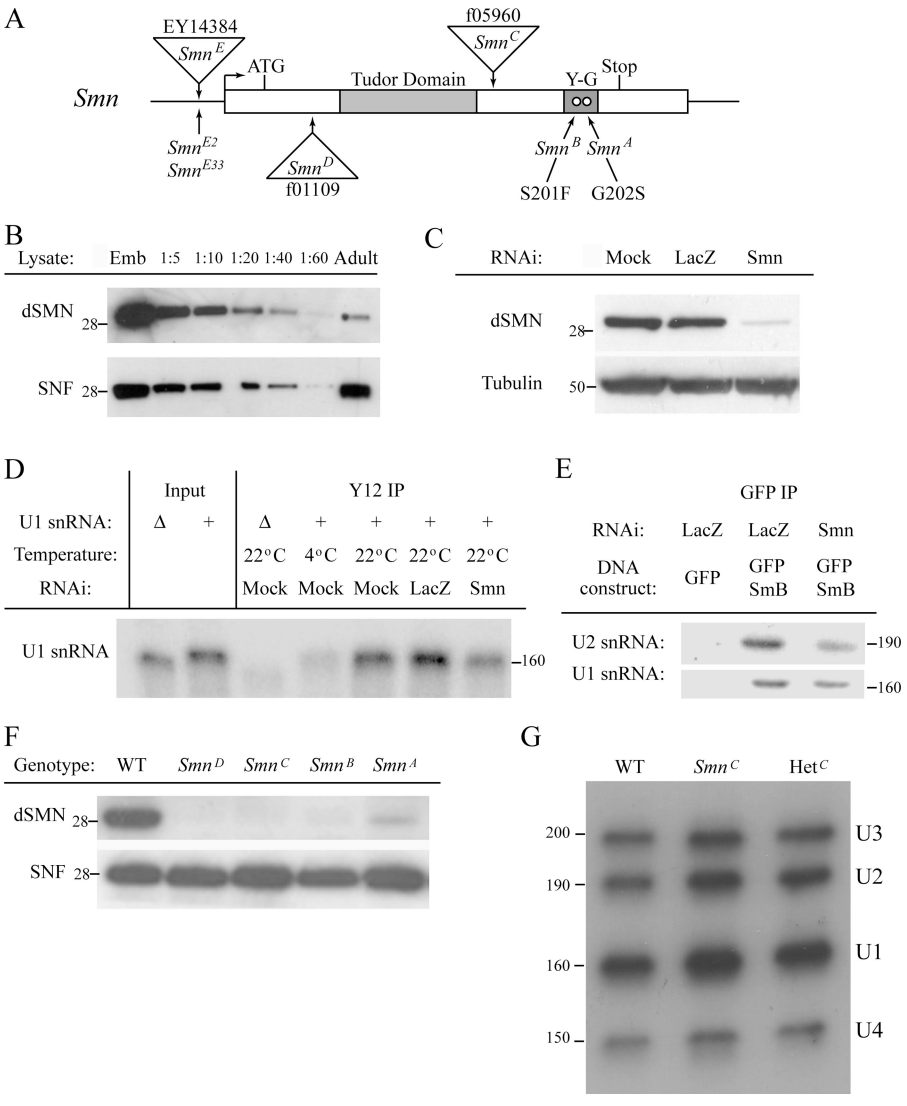

Figure 1. **Genomic architecture and allelic organization of the *D. melanogaster Smn* gene, and its role in snRNP assembly.** (A) *D. melanogaster Smn* is a single-exon gene. Smn^{73Ao} (herein referred to as Smn^A) and Smn^B are missense mutations in the conserved Y-G box described previously (Chan et al., 2003). Transposon insertions are marked by open triangles. Smn^C and Smn^D are piggyBac insertions at +407 and +58 bp from the translation start, respectively. Smn^E is a *P* element insertion at −94 bp, which is upstream of the putative transcription start site. Smn^{E2} and Smn^{E33} are imprecise excision alleles derived from the mobilization of Smn^E. (B) Western blot of embryonic and adult lysates. A dilution series of the embryonic lysate indicated that adults have ∼30-fold less dSMN than embryos. Anti-SNF antibody was used as the loading control. (C) S2 cells were left untreated (Mock) or incubated with dsRNAs targeting either *LacZ* or *Smn*. Cytoplasmic extracts were collected 3 d after treatment, and Western blotting confirmed efficient knockdown of dSMN compared with the loading control. (D) Radiolabeled U1 snRNA transcripts were incubated in cytoplasmic extracts and immunoprecipitated with α-Sm monoclonal antibody Y12 to assay for Sm-core assembly. Incubations of wild-type U1 snRNA (+) at the nonpermissive temperature (4°C) or a U1 construct containing a deletion in the Sm protein binding site (Δ) at the permissive temperature (22°C) served as the negative controls. RNAi knockdown of dSMN significantly disrupted Sm-core assembly compared with mock and *LacZ* dsRNA transfections. (E) After dsRNA treatment for 6 d (two doses of dsRNA), S2 cells were transfected with either GFP alone or GFP-SmB. Immunoprecipitation using anti-GFP antibodies, followed by Northern analysis of U1 and U2 snRNAs, indicated that GFP alone did not bring down detectable amounts of snRNA, the amounts immunoprecipitated by GFP-SmB after RNAi knockdown of dSMN were at least twofold less than in the control (LacZ) knockdown. (F) Expression profile of dSMN in the lethal alleles described in A. All of the lethal alleles are essentially protein nulls, although residual levels of dSMN in lysates derived from the Smn^A and Smn^B alleles varied from preparation to preparation (not depicted). Anti-SNF antibody was used as the loading control. We note that wild-type embryonic lysates were competent for the Sm-core assembly assay shown in D, but larval, pupal, and adult lysates were incompetent, which is consistent with previous results from other species (Gabanella et al., 2005; Wan et al., 2005). (G) Northern blot of total larval RNAs from wild-type (WT), Smn^C homozygous (Smn^C), or heterozygous (Het^C) mutants. 2 μg of RNA were loaded in each lane; comparable levels of U1, U2, and U4 snRNAs were detected (U3 was used as a control). Molecular weight markers are in kilodaltons.

f01109 (Smn^D) are piggyBac insertions within the coding region. Developmental analysis of these mutants demonstrated that Smn^E homozygotes are completely viable, with no apparent phenotype. The Smn^C and Smn^D alleles are late-larval lethals. Genetic complementation studies revealed that the A-D alleles failed to complement each other, and that crossing them over appropriate deletions did not accelerate the lethal phase. Importantly, transgenic expression of a UAS-YFP-*Smn* construct under control of a *daughterless*-GAL4 driver completely rescued the larval lethality of the two alleles we tested, producing viable adults. Thus, the A-D alleles are genetic-null mutants. Consistent with these genetic results, Western blotting of lysates from the phenocritical phase (second to third instar) indicated a complete loss of dSMN protein (Fig. 1 F and not depicted). However, despite the loss of dSMN, we could detect no appreciable differences in spliceosomal snRNA levels in the mutant larvae (Fig. 1 G and Fig. S1, available at http://www.jcb.org/cgi/content/full/jcb.200610053/DC1). These findings are similar to those of Wan et al. (2005), which showed that reduced SMN expression and impaired snRNP synthesis caused a slow growth phenotype, but did not affect steady-state snRNP levels in chicken DT40 cells. Thus, despite the observation that dSMN functions in snRNP biogenesis in *D. melanogaster*, the lethality associated with the null mutants is not caused by a systemic depletion of snRNPs.

Smn hypomorphs: a model for SMA in the adult fly

SMA is caused by reduced levels of SMN in mammals; complete loss of function results in early lethality (Monani, 2005). To generate a better *D. melanogaster* model for SMA, we screened for neuromuscular phenotypes in adult flies by imprecise excision of the *P* element in Smn^E. From a total of ~170 independent excisions, we isolated two lines (Smn^{E2} and Smn^{E33}) that displayed overt motor dysfunction. Smn^{E2} and Smn^{E33} homozygotes (henceforth referred to as E2 and E33 mutants, respectively) each showed marked defects in flying and jumping. The E2 mutants exhibited a 2-d delay in pupation, reflecting an extended larval period, and ~20% of the E2 pupae died at the pharate adult stage. However, the phenotype of the E2 mutants was incompletely penetrant; ~45% of E2 animals had flight and jump defects. Moreover, dSMN expression levels in these animals were also variable (unpublished data). In contrast, E33 mutants were completely viable and fertile, and 100% of the animals were incapable of flying or jumping (Videos 1 and 2, available at http://www.jcb.org/cgi/content/full/jcb.200610053/DC1). Because the E33 phenotype was fully penetrant, this allele was chosen for further characterization.

The indirect flight muscles (IFMs) of the *D. melanogaster* thorax are among the best characterized muscles in the adult animal and are essential for flight (Fernandes and Keshishian, 1999). Because E33 mutants are flightless, we prepared hemithoraces by dissection and analyzed the IFMs of wild-type and mutant animals by light microscopy. The IFMs of the fruitfly are composed of dorsal longitudinal muscles (DLMs) and dorsoventral muscles (DVMs). The mutant IFMs were highly disorganized, even when observed at a gross level (Fig. 2 A). Although DLM fibers in wild-type flies span the entire anteroposterior length of the dorsal thorax, E33 DLMs often failed to extend the whole length of the thorax, and DVMs were typically unidentifiable (Fig. 2 A). When salicylate-cleared thoraces were imaged under plane-polarized light, significant muscle degeneration was apparent in the mutant fibers (Fig. 2 B). Under higher magnification, wild-type IFMs showed the characteristic

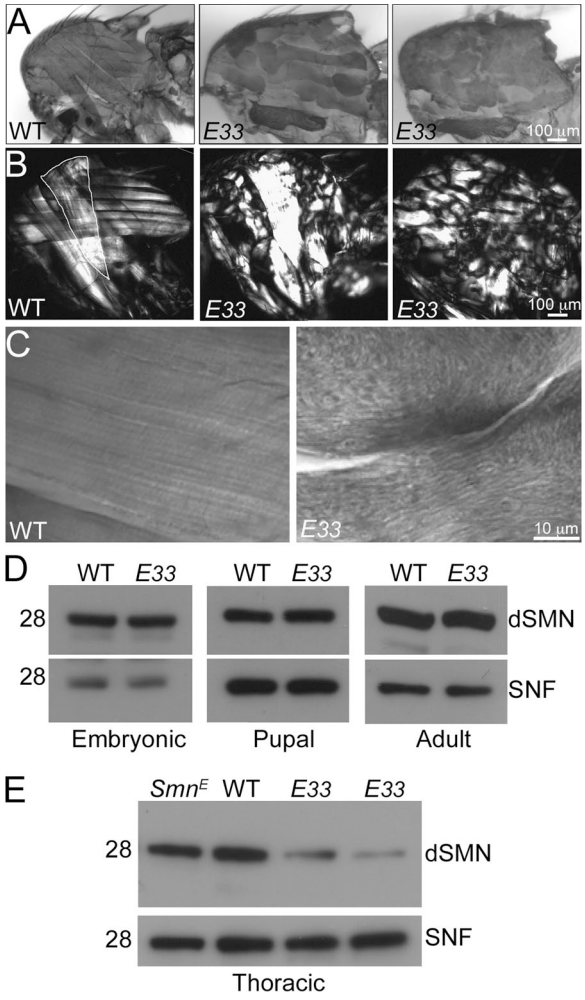

Figure 2. **Phenotypic analysis of Smn^{E33} hypomorphs.** (A) Light microscopic analysis of hemithoraces from 2–3-d-old wild-type (WT, left) and E33 mutant IFMs showed considerable disorganization of muscle fibers (middle and right). (B) Thoraces were visualized under plane-polarized optics after clearing in methylsalicylate. The IFMs consist of two groups, the DLMs and the DVMs. DLMs run from anterior to posterior on the dorsal side of the thorax, and DVMs run dorsoventrally, nearly perpendicular to the DLMs. Wild-type muscles appear normal (left), including the tergal depressor of the trochanter (jump) muscle, outlined in white and below the plane of the DLMs. Mutant fibers showed clear signs of degeneration (dark patches within the muscle). Both DLMs and DVMs were equally and severely affected; however, the jump muscles displayed normal (center) to severe (right) degeneration phenotypes. (C) Higher magnification view of wild-type (WT) and E33 mutant DLMs showing striations in the wild type that are absent from the mutant myofibers. (D and E) Western blotting of dSMN from embryonic, pupal, total adult, or total adult thoracic lysates. Although no major differences in dSMN levels were detected in the total lysates at any of the developmental stages, dSMN was markedly reduced in E33 mutant thoraces (two different preparations are shown) compared with either wild type or the parental Smn^E line. Antibodies against SmB (Y12) and SNF were used as loading controls. Molecular weight markers are in kilodaltons.

striations, whereas the mutant muscles were extremely irregular, with numerous bulges and constrictions throughout (Fig. 2 C). Thus, E33 mutants display severe muscular atrophy, which is one of the hallmark features of SMA.

Genetic complementation analyses revealed that the loss-of-function (null) alleles, described in the previous section (Fig. 1 A), each failed to complement the motor dysfunction phenotype of the E33 allele. Furthermore, the flightlessness of the E33 mutation was rescued by expression of the UAS-YFP-*Smn* transgene under the control of a *daughterless*-GAL4 driver, demonstrating that the observed motor defects in E33 are, indeed, caused by loss of dSMN function. Therefore, we were somewhat surprised when we analyzed developmentally staged lysates by Western blotting of dSMN and found no appreciable differences between adult wild-type and E33 mutants (Fig. 2 D). Upon further analysis, we found that the amount of dSMN produced in the mutant thoraces was substantially reduced relative to either wild-type or Smn^E parental lines (Fig. 2 E). Although the reason for this tissue-specific depletion is currently unknown, the mutants presented us with an opportunity to analyze the neuromuscular defects associated with reduced dSMN expression.

During the embryonic–larval transition, *D. melanogaster* motoneurons contact muscle fibers only after the completion of myogenesis (Johansen et al., 1989). In contrast, adult motoneurons establish contact with the developing muscle fibers during myogenesis, which is a situation more akin to that of vertebrate development (Fernandes and Keshishian, 1999). Fruitfly DLMs are innervated by remodeled larval motoneurons whose cell bodies lie within the thoracic ganglion and project dorsally into the flight muscles (Fernandes and Keshishian, 1999). Using monoclonal antibody 22C10, which stains neuronal processes (Patel, 1994), we analyzed the DLMs of E33 hypomorphs for defects in the organization of their DLM motoneurons. As shown in Fig. 3, both the number and routing of primary motoneuron branches was clearly compromised in E33 flies, as compared with controls. Secondary branches were disorganized (Fig. 3) and arborization defects ranged from moderate to severe. Because the mutant muscle fibers were spatially disorganized, it was difficult to assign parameters to the individual motoneurons. Using criteria established by Hebbar and Fernandes (2004) as a guide, we scored flies from each genotype and found that ∼80% of the mutant thoraces showed motoneuron routing defects; a smaller fraction (∼40%) showed defects in secondary branching and arborization. No such defects were observed in the control animals. Thus, we conclude that reduced thoracic *Smn* expression leads to acute neuromuscular dysfunction in *D. melanogaster*.

Smn is required for *Actin88F* expression

The development of muscles and motoneurons in the adult fruitfly are spatiotemporally associated. In other words, the synthesis of structural proteins important for one tissue can require the presence of the other tissue. For example, formation of the male-specific muscle (MSM) and the development of its specialized characteristics are absolutely dependent on innervation

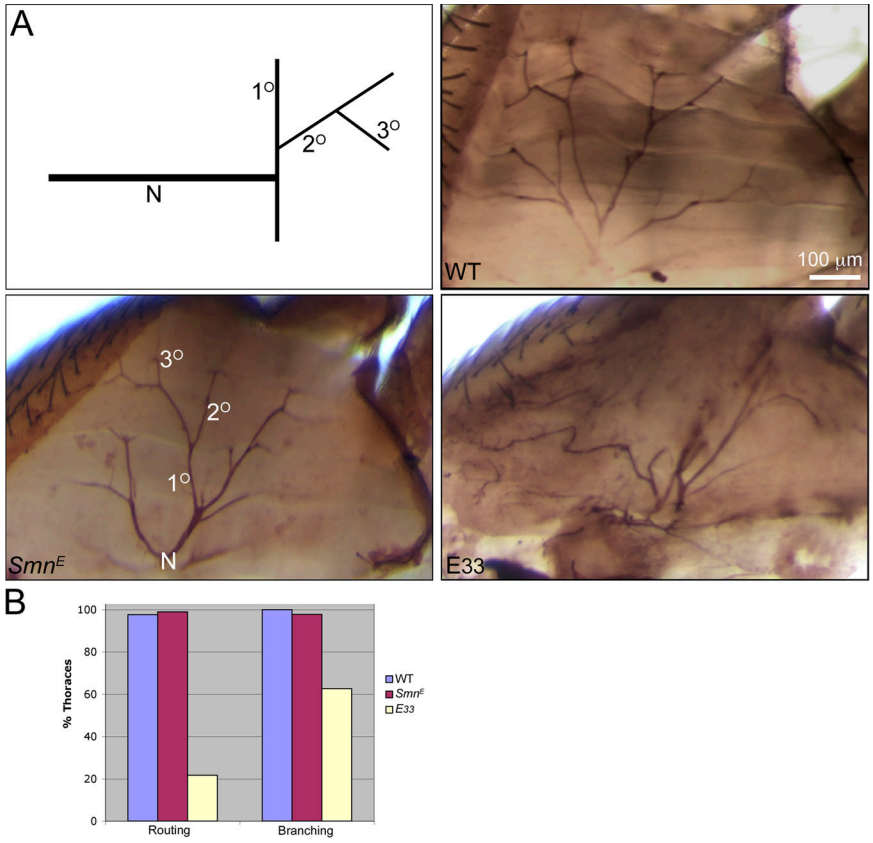

Figure 3. **DLM motoneuron organization in E33 mutants.** (A) Schematic of motoneuron branching pattern in adult DLMs. Primary branches (1°) grow out from the main nerve trunk (N) that traverses the length of the six adult DLM fibers. Defasciculation of primary branches leads to establishment of secondary (2°) and tertiary (3°) branches, which develop the terminal arbor (not depicted). DLM motoneurons were stained with monoclonal antibody 22C10, which stains neuronal processes. Organization of primary branches in both the wild-type and the parental Smn^E animals appeared normal. The number and routing of primary motoneuron branches were severely compromised in E33 flies. (B) Quantitation of routing and branching defects in wild-type and mutant DLMs. Primary branches that displayed a meandering path were taken as having routing defects. Motoneurons displaying fewer than three secondary branches were scored as having a secondary branching defect (wild-type animals display a minimum of four to five secondary branches). 90 hemithoraces (from 90 individual flies) of each genotype were scored.

(Currie and Bate, 1995). Furthermore, expression of an MSM-specific actin isoform, Act79B, is also dependent on innervation (Currie and Bate, 1995). Similarly, in vertebrates, denervation is known to result in reduced expression of skeletal muscle actin (Shimizu et al., 1988). Given that SMA is characterized by motoneuron denervation, it seemed likely that the neuromuscular defects observed in the E33 hypomorphs was also coupled with innervation failure. Because one of the hallmarks of innervation failure is reduced expression of actin, we tested whether the IFM-specific actin isoform Act88F (Fyrberg et al., 1983) was expressed in the *Smn* hypomorphs. RT-PCR was performed on thoracic RNA from wild-type, Smn^E, and E33 animals, using primers specific for *Act88F*, *Tropomyosin 2 (Tm2)*, and *Troponin I (TnI)* transcripts. Expression of *Act88F* was undetectable in the mutant thoraces, whereas the transcripts were easily detected in the wild-type and Smn^E strains (Fig. 4 A). We note that loss of *Act88F* expression was not caused by a general loss of transcription or splicing in the IFMs, as the RT-PCR products for *TnI* and *Tm2* (which cross intron–exon boundaries) were comparable in all three samples (Fig. 4 A). Consistent with the idea that splicing is unaffected in the mutants, Northern analysis of thoracic lysates from wild-type or E33 flies showed no significant differences in steady-state levels of either snRNAs (Fig. 4 B) or trimethylguanosine-capped snRNPs (Fig. S1). Staining of wild-type (Fig. 4 C) and mutant (Fig. 4 D) muscles with phalloidin confirmed the general loss of filamentous actin in the hypomorphic IFMs. Most importantly, actin staining and proper myofibril formation were rescued by transgenic expression of YFP-dSMN (Fig. 4 E). Thus, reduced levels of dSMN protein result in loss of Act88F expression and severe neuromuscular disorganization.

SMN interacts with α-actinin

In a parallel set of experiments, we were interested in purifying and characterizing the *D. melanogaster* SMN complex. After transient transfection of S2 cells with a Flag-dSMN construct, we performed a pulldown experiment with anti-Flag beads. Associated proteins were eluted from the beads by boiling in sample buffer and subjected to SDS-PAGE. The protein profiles of transfected versus nontransfected cells were compared by

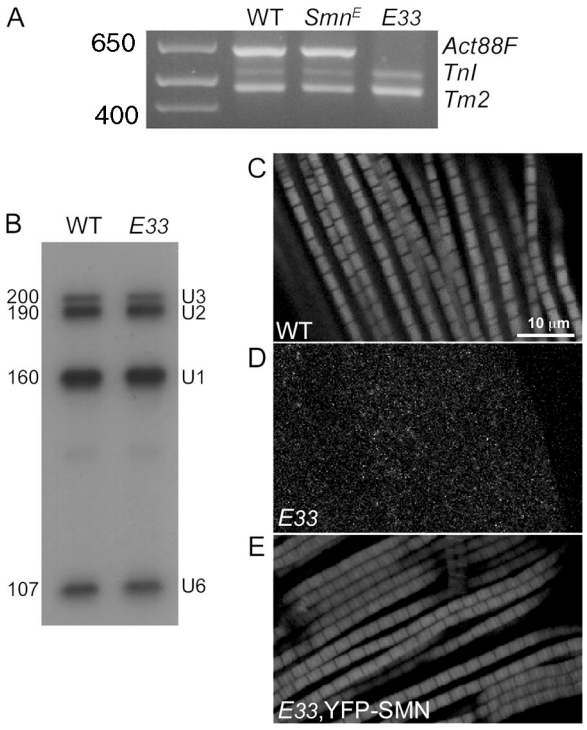

Figure 4. **Thin, but not thick, filament formation is compromised in E33 mutant IFMs.** (A) RT-PCR analysis of IFM-specific actin (Act88F) expression; transcripts were not detectable in E33 mutants, whereas expression was normal in the wild-type (WT) and the parental Smn^E alleles. Troponin I (TnI) and tropomyosin 2 (Tm2) RT-PCR products served as internal controls. (B) Northern blot of total thoracic RNA from adult wild-type (WT) or E33 mutants shows that steady-state U1 and U2 snRNA levels are normal. U3 and U6 snRNA levels used as loading controls. 2 μg of total RNA were loaded in each lane. (C–E) Loss of actin expression was confirmed in E33 mutant myofibers using phalloidin. Whereas the characteristic repetitive blocks of actin were observed in wild-type (WT) myofibrils (c), no staining was detected in the mutant (d). Actin staining in the E33 mutants was restored by transgenic expression of YFP-dSMN (E). Molecular weight markers in base pairs.

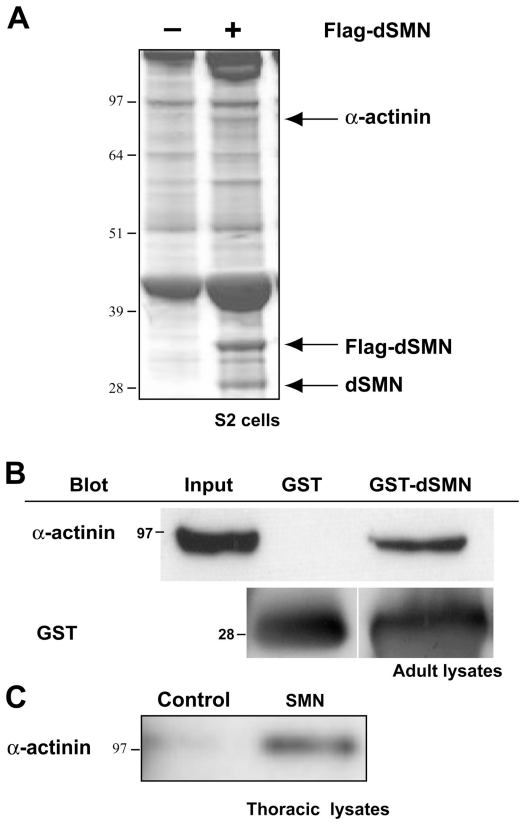

Figure 5. ***D. melanogaster* SMN forms a complex with α-actinin.** (A) Flag-dSMN was transiently transfected into S2 cells and purified over anti-FLAG beads. Eluted proteins were subjected to SDS-PAGE and Coomassie staining. Untransfected cells were used as a negative control. The three marked bands were excised from the gel and identified by mass spectrometry as α-actinin, Flag-dSMN, and dSMN, respectively. (B) Pulldown assays with GST-dSMN or GST alone were performed using total adult lysates. The pulldowns were assayed by Western blotting with monoclonal α-actinin antibodies. Polyclonal anti-GST antibodies were used for the loading controls. (C) Proteins were coimmunoprecipitated from adult thoracic lysates with dSMN antibodies and analyzed by Western blotting with α-actinin antibodies. Molecular weight markers in kilodaltons.

Coomassie staining (Fig. 5 A). Although a more detailed analysis (unpublished data) suggests that there are likely to be many other differences between the two samples, three prominent bands could be easily distinguished. The bands were excised from the gel and analyzed by mass spectrometry. The two smaller proteins were identified as Flag-dSMN and endogenous dSMN (Fig. 5 A and not depicted). Because SMN is known to self-oligomerize (Lorson et al., 1998), we expected to recover the endogenous dSMN protein. However, the third, ~100-kD band was identified by 39 distinct peptides in the mass spectrogram as *D. melanogaster* α-actinin (Fig. S2, available at http://www.jcb.org/cgi/content/full/jcb.200610053/DC1).

Because α-actinin is a protein known to play a major role in cross-linking actin filaments within numerous cell types, including muscle (Clark et al., 2002), we tested whether dSMN interacts with α-actinin in additional biochemical assays. We performed GST-pulldown and coimmunoprecipitation analyses using adult and thoracic lysates. Fig. 5 B shows that α-actinin was recovered using GST-dSMN, but not with GST alone (control). As shown in Fig. 5 C, anti-dSMN antibodies weakly, but reproducibly, coprecipitated α-actinin. Control (anti-myc) antibodies and beads coprecipitated only background amounts of α-actinin. Collectively, these studies show that dSMN forms a complex with α-actinin in vivo.

SMN localizes to IFM myofibrils

Given the aforementioned findings, we analyzed the localization of dSMN in the IFMs of wild-type and YFP-dSMN transgenic flies (Fig. 6). Each IFM myofiber is a single multinucleate cell composed of several myofibrils that contain numerous functional units called sarcomeres. Within each sarcomere, actin (thin) and myosin (thick) filaments interdigitate to form contractile elements. Thick filaments are anchored together within a structure known as the M-line, whereas thin filaments are anchored at the Z-line or Z-disc (Clark et al., 2002). The region between the M-lines is called the I-band. Actin is typically excluded from the M-line, localizing throughout the I-band, and it is often enriched at, or depleted from, the Z-line.

In wild-type and YFP-dSMN transgenic myofibers, dSMN was detected not only in muscle cell nuclei but also in the individual myofibrils (Fig. 6, E and F; and not depicted). Within the myofibrils, three distinct patterns of sarcomeric localization were observed: I-band, Z-line enriched, and granular (Fig. 6, A–C). The same three SMN localization patterns were visible in IFM myofibrils from YFP-dSMN transgenic flies (Fig. 6, J–L). The I-band pattern was the predominant one, as confirmed by phalloidin costaining (Fig. 6, G–I). However, the dSMN and actin staining patterns did not always correlate, especially in respect to accumulation at the Z-line. That is, when actin was

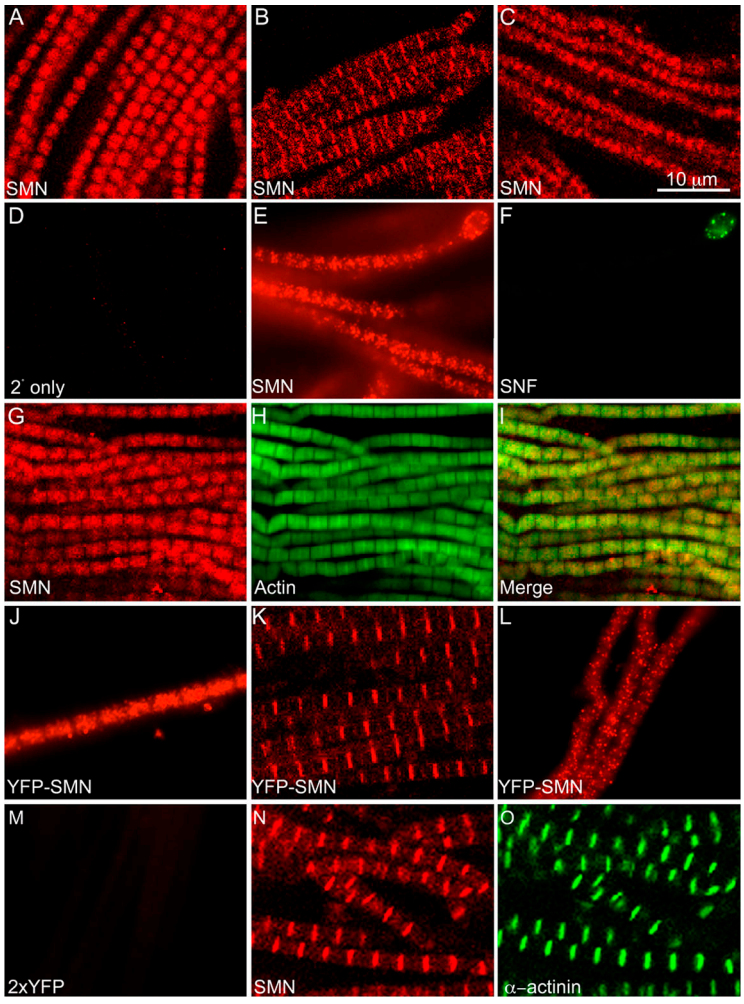

Figure 6. **Sarcomeric localization of dSMN in wild-type and YFP-dSMN transgenic IFM myofibrils.** (A–C) Three patterns of dSMN localization (I-band [A], Z-line enriched [B], and granular [C]) were observed using affinity-purified anti-dSMN antibodies. (D) Control image using secondary antibody only (2° only). (E and F) Control images showing that dSMN localizes to both nuclei and myofibrils, whereas anti-SNF (a spliceosomal protein) antibodies stain only nuclei. (G–I) Costaining of dSMN (red, G) and filamentous actin (green, H) showing dSMN in the I-band pattern. Merged image shown in I. (J–L) The same three patterns observed in A–C were also found in transgenic flies expressing YFP-dSMN (red). (M) Control image of myofibrils from transgenic flies expressing 2xYFP. (N and O) Wild-type myofibrils showing colocalization of dSMN (N) with the Z-line marker α-actinin (O).

enriched at the Z-line, dSMN did not necessarily show a similar enrichment, and vice versa. It is possible that dSMN localization within the sarcomere is dynamic; future experiments will be required to address this point. Meanwhile, control antibodies and secondary antibodies alone clearly failed to stain the sarcomeres (Fig. 6, D and F). Similarly, a 2xYFP transgene construct showed only background staining in the myofibrils (Fig. 6 M). Importantly, in myofibrils where dSMN was enriched at the Z-line, it colocalized with α-actinin (Fig. 6, N and O). We conclude that dSMN localizes to flight muscle sarcomeres.

Smn hypomorphs phenocopy *Act88F*-null mutants

The studies detailed in the previous sections suggested that the flightlessness associated with the Smn^{E33} allele might be caused by a loss of actin expression in the IFMs. Therefore, we examined the IFMs of flies that contain a null mutation in *Act88F* (Okamoto et al., 1986), which is called KM88. Like Smn^{E33} mutants, $Act88F^{KM88}$ homozygotes are flightless and fail to form proper IFMs, but are otherwise viable and fertile (Okamoto et al., 1986). As shown in Fig. 7 A, KM88 mutants express dSMN, but the protein is delocalized. Similarly, α-actinin, an actin filament cross-linking factor (Otey and Carpen, 2004), was mislocalized in both the *Smn* and the *Act88F* mutant backgrounds, which is consistent with a complete failure to form thin filaments.

Further analysis demonstrated that thick filament formation was largely unperturbed in the *Smn* hypomorphic IFMs, and that α-actinin staining did not overlap with the myosin filaments (Fig. 7 B). This scenario is, again, very similar to that of the KM88 mutation, wherein the vast majority of myosin-positive filaments are devoid of α-actinin (unpublished data). Collectively, these findings indicate that dSMN and Act88F are required for proper formation of flight-muscle myofibrils.

Smn localization to sarcomeres is evolutionarily conserved

To determine whether the sarcomeric localization of SMN is a conserved feature among vertebrates, we prepared myofibrils from mouse hindlimb muscles and analyzed the distribution of Smn and α-actinin. As shown in Fig. 8, Smn colocalizes with α-actinin in a Z-line pattern. Two independent anti-SMN antibodies revealed the same pattern, and control antibodies were negative (Fig. 8). Unlike the situation in the fly, mouse Smn localized exclusively to the Z-line; no granular or I-band like patterns were observed.

In summary, four lines of evidence demonstrate that SMN is a bona fide sarcomeric protein. First, localization to the sarcomere was not simply caused by cross-reactivity of the antibodies, as transgenic expression of YFP-dSMN showed prominent myofibrillar staining that was completely absent in control IFMs (Fig. 6). Second, control antibodies fail to stain the sarcomeres of both flies and mice (Figs. 6 and 8). Third, dSMN staining was lost in the E33 mutants, resulting in a loss of *Act88F* expression and thin filament formation (Fig. 4). Fourth, dSMN interacts with α-actinin in vitro and in vivo (Fig. 5), and reduced dSMN expression leads to complete disorganization of α-actinin in situ (Fig. 7 B). Thus, we conclude that SMN is a sarcomeric protein.

Discussion

SMN and the etiology of SMA

Despite the well-established gene–disease relationship between *SMN1* and SMA, the connection between protein function and molecular etiology has been obscured by a plethora of putative cellular functions attributed to SMN (Briese et al., 2005; Eggert et al., 2006). Previous investigations have shown that the SMN

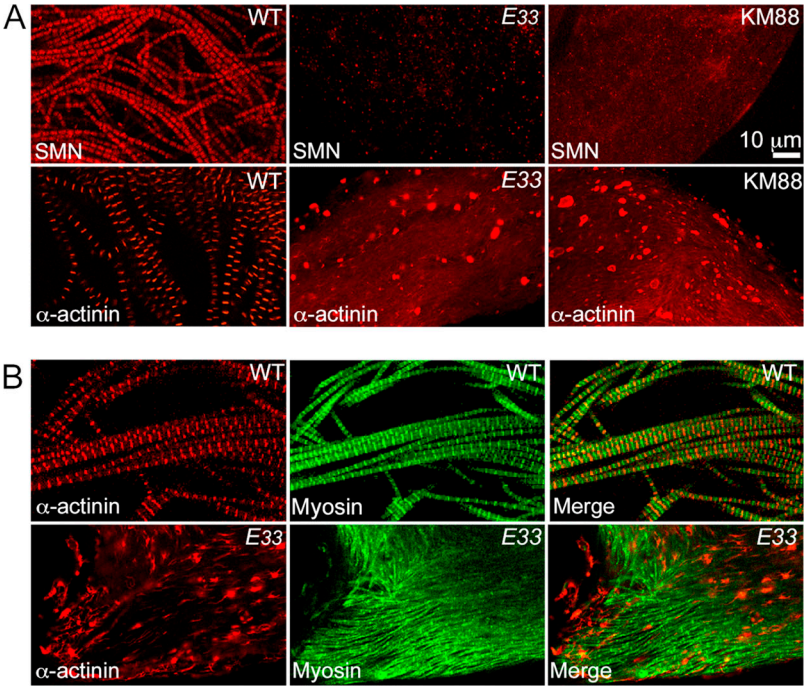

Figure 7. **Localization of dSMN, α-actinin, and myosin in wild-type and mutant IFM myofibrils.** (A) Wild-type (WT, left), *Smn* hypomorphic (E33, middle), and *Act88F*-null mutant (KM88, right) myofibers were stained with anti-dSMN (top) or α-actinin (bottom) antibodies. (B) Staining with α-actinin (red) and myosin (green) antibodies showing thin filament formation is disrupted in E33 mutants (bottom) compared with wild-type controls (top). Thick filaments (green) were detectable in the mutant myofibers (bottom).

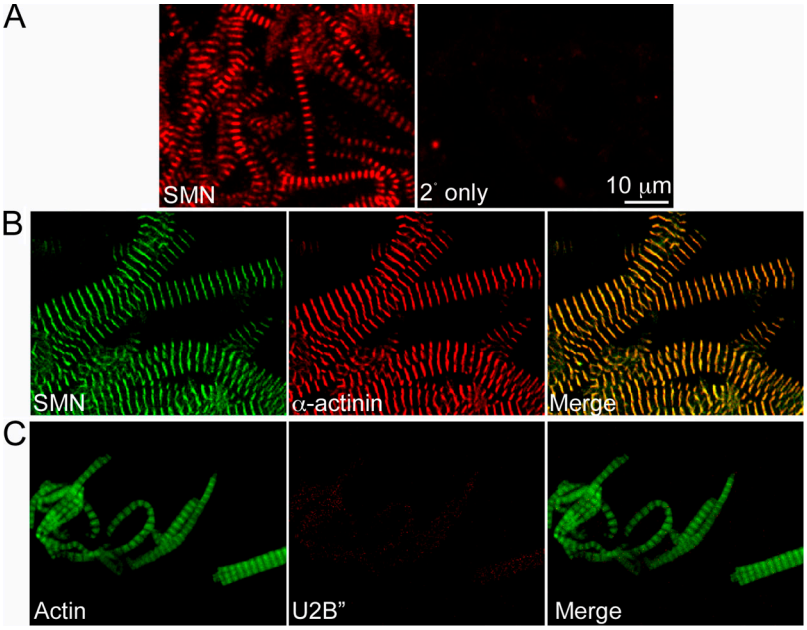

Figure 8. **The sarcomeric localization of SMN is conserved in mouse myofibrils.** (A) SMN localizes in a striated pattern in purified mouse skeletal muscle myofibrils (red, left); the secondary antibody alone (goat anti–mouse Alexa Fluor 594) did not give a specific signal (red, right). (B) The Z-line marker protein, α-actinin (red, center), colocalizes with SMN, as revealed by FITC-conjugated anti-SMN primary antibodies (green, left). (C) As another negative control, an antibody against spliceosomal protein U2B′′ (center, red) showed only faint background staining. Myofibrils were counterstained for actin using FITC-conjugated phalloidin (green, left). (B and C) Merged images are shown on the right.

complex is required for assembly and transport of spliceosomal snRNPs (Fischer et al., 1997; Meister et al., 2001; Pellizzoni et al., 2002; Narayanan et al., 2004; Shpargel and Matera, 2005). Additional findings point to roles for this complex in neurite outgrowth and pathfinding (Fan and Simard, 2002; McWhorter et al., 2003; Sharma et al., 2005), neuromuscular junction formation (Chan et al., 2003), profilin binding (Giesemann et al., 1999; Sharma et al., 2005), and axonal transport of β-actin mRNPs (Rossoll et al., 2003). A common link between each of these additional studies is the actin cytoskeleton. Our finding that reduced dSMN expression leads to motor axon routing and arborization defects, coupled with a loss of Act88F expression in the muscle, is consistent with this actin-related theme.

A muscle-specific function for SMN

The vast majority of SMA studies continue to be focused on a motoneuron-specific role for SMN; our results do not exclude such a function. However, the idea that SMN might also have a muscle-specific function is not a new one. Cocultures of SMA type I and II muscles with wild-type motoneurons failed to sustain innervation, whereas muscles from control or SMA type III patients maintained stable connections, suggesting a muscle-specific requirement for SMN (Braun et al., 1995; Guettier-Sigrist et al., 2002). Similarly, down-regulation of *Smn* in mouse C2C12 cells revealed defects in myoblast fusion (Shafey et al., 2005) and tissue-specific knockouts of *Smn* in mouse muscle resulted in pronounced dystrophic phenotypes (Cifuentes-Diaz et al., 2001; Nicole et al., 2003). Also in support of a muscle-specific function is the observation that, despite having comparable levels of SMN, mouse skeletal muscle extracts failed to support efficient Sm-core assembly, whereas extracts from spinal cord were quite active (Gabanella et al., 2005). Collectively, these studies show that relatively high levels of SMN are required in muscles, although the reason for this requirement was unclear.

Our discovery that SMN is a sarcomeric protein required for expression of muscle-specific actin not only provides a plausible role for the protein in muscles, but highlights the potential importance of this tissue in SMA pathophysiology. At least 20 different skeletal muscle diseases are thought to be caused by mutation or mislocalization of sarcomeric proteins (Sarnat, 1992; Hauser et al., 2000; Moreira et al., 2000; Selcen and Engel, 2003; Laing and Nowak, 2005). In this regard, it is particularly interesting that SMA patients have been shown to display varying degrees of myofibrillar/sarcomeric (including Z-line) abnormalities (Szliwowski and Drochmans, 1975; Braun et al., 1995). Notably, αB-crystallin was recently reported to form a complex with SMN in HeLa cells (den Engelsman et al., 2005). αB-crystallin is an intermediate filament protein that, in muscle cells, accumulates at the Z-line (Laing and Nowak, 2005). Thus, the SMN complex can interact with at least two distinct Z-line proteins, α-actinin, and αB-crystallin.

We have shown that reduced thoracic dSMN levels result in loss of Act88F expression with no apparent defect in either snRNP biogenesis or pre-mRNA splicing. Because expression of muscle-specific actin is known to be dependent on motoneuron innervation (Shimizu et al., 1988; Currie and Bate, 1995), the neuronal defects observed in the Smn^{E33} hypomorphs are consistent with those expected of an SMA model. Further, the data are consistent with denervation as either the cause or a consequence of muscle degeneration. Notably, a fraction of SMA type III patients display dystrophic phenotypes without evidence of neurogenic abnormalities (Szliwowski and Drochmans, 1975; Vajsar et al., 1998; Muqit et al., 2004). Although motoneuron loss is generally regarded as a late event in disease progression, one of the main problems in studying SMA, especially the severe forms, is that we are only able to analyze the end-stage of the disease.

We currently do not know whether the mutant phenotype observed in the *Smn* hypomorphs is caused by reduced dSMN

expression in the thoracic muscles, the motoneurons, or a combination of tissues. Future work using tissue-specific rescue constructs and a detailed analysis of motoneuron development and myogenesis in the *Smn* hypomorphic pupae will address these important issues. Regardless of the actual disease trigger, the identification of SMN as a sarcomeric protein underscores the importance of muscle cell function in modulating the severity of SMA.

Materials and methods

Fly stocks and genetics

Oregon-R was used as the wild-type allele. Missense alleles Smn^{A} and Smn^{B} were gifts from M. van den Heuvel (Oxford University, Oxford, UK). Transposon insertion alleles Smn^{C} (f05960) and Smn^{D} (f01109) were obtained from the Exelixis collection at Harvard Medical School. Smn^{E} (EY14384) was a gift from H. Bellen (Baylor College of Medicine, Houston, TX; Bellen et al., 2004). Excision alleles were generated by mobilization of the Smn^{E} *P* element using standard protocols. KM88 was a gift from J. Vigoreaux (University of Vermont, Burlington, VT). All stocks were cultured on standard cream-of-wheat agar at room temperature (24 ± 1°C) in half-pint bottles. Genetic complementation analyses were performed using standard methods. *UAS*-2xEYFP, which was used as control for nonspecific localization, and the *daughterless-Gal4* (*da-Gal4*) lines were obtained from the Bloomington Stock Center. For rescue experiments, a YFP-dSMN transgene (a gift from J. Gall, Carnegie Institution of Washington, Baltimore, MD) was expressed under the control of *da-Gal4* in the following homozygous backgrounds: Smn^{E33}, Smn^{A}, and Smn^{B}.

Western blotting

Embryonic, larval, adult (total and thoracic), and S2 cell lysates were prepared, electrophoresed, and blotted using standard protocols. Anti–rabbit dSMN antibody (a gift from J. Zhou, University of Massachussetts Medical School, Worcester, MA) was affinity-purified and used at a dilution of 1:10,000. Antibodies against SNF (4G3, monoclonal), SmB (Y12, monoclonal), and tubulin (anti–rabbit; Sigma-Aldrich) were used as loading controls. Appropriate HRP-conjugated secondary antibodies were used for detection.

snRNP assembly assay

Smn and *LacZ* dsRNAs were transcribed in vitro from PCR products flanked with T7 promoters. *D. melanogaster* S2 cells were placed in SF-900 media containing 14 μg/ml of dsRNA. Extracts were generated 3 d after dsRNA treatment using the Ne-Per nuclear/cytoplasmic extraction kit (Pierce Chemical Co.) and dialyzed in reconstitution buffer (20 mM Hepes-KOH, pH 7.9, 50 mM KCl, 5 mM $MgCl_2$, and 0.2 mM EDTA) as previously described (Pellizzoni et al., 2002). 40 μg of cytoplasmic extract were loaded on a gel for Western blotting to confirm knockdown. For the assembly assay, wild-type *D. melanogaster* U1 snRNA and U1 snRNA containing a deletion of the Sm assembly site were in vitro transcribed from PCR products in the presence of [^{32}P]UTP and m7G cap analogue (Promega). 100,000 counts of radiolabeled U1 snRNA were incubated in 100 μg of cytoplasmic extract at 22°C for 40 min in reconstitution buffer. Assembled snRNPs were precleared with protein G beads before immunoprecipitation with monoclonal antibody Y12 in RSB-100 buffer (600 mM NaCl, 20 mM Tris-HCl, pH 7.4, 2.5 mM $MgCl_2$, and 0.01% NP-40; Pellizzoni et al., 2002). Immunoprecipitated RNAs were denatured in formamide loading buffer, run on a 6% acrylamide TBE-urea gel, and exposed to a phosphorimager.

GST pulldown assay

GST-dSMN was cloned as previously described (Ilangovan et al., 2003). Total fly lysate was homogenized in NET buffer (150 mM NaCl, 50 mM Tris, pH 7.5, and 5 mM EDTA). 500 μg of lysate was passed over recombinant 8 μg GST or GST-dSMN beads overnight in NET buffer. The pulldown products were washed and loaded on a denaturing gel.

IP-Northern

15 μg of dsRNA against *Smn* or *LacZ* (control) were added twice to S2 cell medium over a course of 6 d. After knockdown, cells were transfected with GFP-SmB. Northern blotting of GFP-SmB immunoprecipitate using radiolabeled *D. melanogaster* U1 and U2 snRNA probes was performed following established protocols.

Northern blotting

Total RNA from adult thoraces was extracted using TRIZOL (Invitrogen). Adult thoraces were pulled apart from the main body, and wings and legs were clipped close to the thorax. Thoraces were immediately transferred to TRIZOL and homogenized. Total RNA was extracted following the manufacturer's instructions. RNA was run on a standard 10% polyacrylamide-urea gel (Invitrogen), transferred to a nylon membrane, and probed with ^{32}P-labeled PCR products corresponding to the *D. melanogaster* U1, U2, and U6 snRNAs and U3 snoRNA.

RT-PCR

Total RNA from adult thoraces was prepared as described in the previous section. RT-PCR, with appropriate controls, was performed using SuperScript First-Strand synthesis system (Invitrogen). In brief, oligo-dT–primed first-strand synthesis products were subjected to 20 cycles of PCR using gene-specific primers. Sequences are as follows: Act88F, sense 5′-CCACGCCATTCTGCGTCTGG-3′ and antisense 3′-GCTGCCTTTGAAGAGCTTTCGCG-3′; troponin I, sense 5′-TTGTGAAGGCCAGAAATGGG-3′ and antisense 5′-GACTTCATTTCTGATCAAAT-CCAT; and tropomyosin 2, sense 5′-CACCATGGACGCCATCAAGAAG-3′ and antisense 5′-TTGGTATCGGCATCCTCAGC-3′.

Immunostaining

The IFMs were dissected from the thorax with the help of fine forceps and needles in a drop of PBS. The entire muscle preparation was fixed in 4% paraformaldehyde, and the fibers were partially teased apart with needles. Immunofluorescence was performed following established protocols. Certain preparations were also stained for filamentous actin by adding 1 μM FITC-conjugated phalloidin (Sigma-Aldrich) 20 min before the secondary antibody incubation was completed. Images were taken using either a TCS SP2 laser scanning confocal microscope or a DM6000 microscope (both Leica), and assembled using Photoshop (Adobe). The Leica Confocal Scanner is interfaced with Leica Confocal Software, and the DM6000 microscope is interfaced with Volocity software. Images were captured at room temperature using a 62× oil immersion objective.

YFP-dSMN localization

Wild-type and transgenic thoracic muscles were dissected in a drop of phosphate-buffered saline (PBS) and fixed in 4% paraformaldehyde. Certain preparations were stained with 1 μM TRITC-phalloidin for 20 min to reveal filamentous actin. Teased myofibrils were washed in PBS and mounted in antifade (50% glycerol and 2.3% 1,4-diazobicyclo-2,2,2-octane). Images were obtained using a TCS SP2 laser scanning confocal microscope or DM6000 microscope, and assembled using Photoshop.

Motoneuron staining

Hemithoraces were generated by freezing in liquid nitrogen and dissecting with a razor blade along the central axis of the body. The bisection was slightly offset from the midline, so as to preserve the other half of the thorax intact. Tissues were then processed for immunostaining essentially as previously described (Hebbar and Fernandes, 2004). During fixation, IFMs of the bisected side were flipped over to expose the contralateral hemithorax. The routing of the primary axons and the number of secondary branches was quantitated as described in the text.

Analysis of IFMs

Hemithoraces were prepared as described in the previous section, and the thoraces were observed and imaged under bright-field optics, with or without counterstaining with safranin for contrast. Analysis of muscles using plane-polarized optics was performed essentially as previously described (Nongthomba and Ramachandra, 1999).

Preparation and staining of mouse myofibrils

Mouse skeletal myofibrils were prepared by the method of Knight and Trinick (1982). In brief, hind leg skeletal muscles were depleted of calcium by incubating in an EGTA–Ringer's solution overnight at 4°C. The sample was placed in rigor buffer and homogenized using a glass Dounce tissue grinder. The homogenate was spun (2,000 *g* for 5 min) and washed in repeated cycles until a pure preparation of myofibrils (as monitored by phase-contrast microscopy) was obtained. Purified myofibrils were adsorbed onto a gelatin-coated slide and subjected to immunofluorescence analysis using standard protocols. Note that for dual staining of Smn and α-actinin, mouse monoclonal antibodies targeting α-actinin were incubated with the purified myofibrils, followed by incubation with secondary antibodies conjugated to Alexa Fluor 594. After extensive washes,

the preparations were incubated with FITC-conjugated monoclonal anti-SMN antibodies.

Online supplemental material

Fig. S1 shows the analysis of snRNA and snRNP levels in wild-type and mutant animals. Fig. S2 shows the amino acid sequence of *D. melanogaster* α-actinin that was covered by mass spectrometric analysis of the band shown in Fig. 5 A. Videos 1 and 2 show the flight behavior of wild-type and E33 mutant adult flies, respectively. The online version of this article is available at http://www.jcb.org/cgi/content/full/jcb.200610053/DC1.

We thank D. Kiehart, J. Saide, and J. Zhou for antibodies, M. Kinter for mass spectrometric analyses, and H. Bellen, J. Gall, M. van den Heuvel, J. Vigoreaux, and the Bloomington and Harvard/Exelixis stock centers for fly lines. We are particularly grateful to B. Dabagh for assistance with the *P* element mobilization crosses. The 22C10 monoclonal antibody developed by S. Benzer was obtained from the Developmental Studies Hybridoma Bank under the auspices of the National Institute of Child Health and Human Development and maintained by the Department of Biological Sciences at the University of Iowa.

This work was supported by National Institutes of Health (NIH) grants R01-GM53034 and R01-NS41617. T.K. Rajendra was supported in part by a grant from Families of Spinal Muscular Atrophy. K.B. Shpargel and M.P. Walker were supported in part by NIH predoctoral traineeships T32-GM08613. G.B. Gonsalvez was supported in part by an NIH postdoctoral traineeship, T32-HD07104. Microscopy support was provided by NIH grants S10-RR021228 and S10-RR017980.

Submitted: 12 October 2006
Accepted: 6 February 2007

References

Bellen, H.J., R.W. Levis, G. Liao, Y. He, J.W. Carlson, G. Tsang, M. Evans-Holm, P.R. Hiesinger, K.L. Schulze, G.M. Rubin, et al. 2004. The BDGP gene disruption project: single transposon insertions associated with 40% of *Drosophila* genes. *Genetics*. 167:761–781.

Braun, S., B. Croizat, M.C. Lagrange, J.M. Warter, and P. Poindron. 1995. Constitutive muscular abnormalities in culture in spinal muscular atrophy. *Lancet*. 345:694–695.

Briese, M., B. Esmaeili, and D.B. Sattelle. 2005. Is spinal muscular atrophy the result of defects in motor neuron processes? *Bioessays*. 27:946–957.

Chan, Y.B., I. Miguel-Aliaga, C. Franks, N. Thomas, B. Trulzsch, D.B. Sattelle, K.E. Davies, and M. van den Heuvel. 2003. Neuromuscular defects in a *Drosophila* survival motor neuron gene mutant. *Hum. Mol. Genet.* 12:1367–1376.

Cifuentes-Diaz, C., T. Frugier, F.D. Tiziano, E. Lacene, N. Roblot, V. Joshi, M.H. Moreau, and J. Melki. 2001. Deletion of murine SMN exon 7 directed to skeletal muscle leads to severe muscular dystrophy. *J. Cell Biol.* 152:1107–1114.

Clark, K.A., A.S. McElhinny, M.C. Beckerle, and C.C. Gregorio. 2002. Striated muscle cytoarchitecture: an intricate web of form and function. *Annu. Rev. Cell Dev. Biol.* 18:637–706.

Courseaux, A., F. Richard, J. Grosgeorge, C. Ortola, A. Viale, C. Turc-Carel, B. Dutrillaux, P. Gaudray, and J.L. Nahon. 2003. Segmental duplications in euchromatic regions of human chromosome 5: a source of evolutionary instability and transcriptional innovation. *Genome Res.* 13:369–381.

Currie, D.A., and M. Bate. 1995. Innervation is essential for the development and differentiation of a sex-specific adult muscle in *Drosophila melanogaster*. *Development*. 121:2549–2557.

den Engelsman, J., D. Gerrits, W.W. de Jong, J. Robbins, K. Kato, and W.C. Boelens. 2005. Nuclear import of {alpha}B-crystallin is phosphorylation-dependent and hampered by hyperphosphorylation of the myopathy-related mutant R120G. *J. Biol. Chem.* 280:37139–37148.

Eggert, C., A. Chari, B. Laggerbauer, and U. Fischer. 2006. Spinal muscular atrophy: the RNP connection. *Trends Mol. Med.* 12:113–121.

Fan, L., and L.R. Simard. 2002. Survival motor neuron (SMN) protein: role in neurite outgrowth and neuromuscular maturation during neuronal differentiation and development. *Hum. Mol. Genet.* 11:1605–1614.

Fernandes, J.J., and H. Keshishian. 1999. Development of the adult neuromuscular system. *Int. Rev. Neurobiol.* 43:221–239.

Fischer, U., Q. Liu, and G. Dreyfuss. 1997. The SMN-SIP1 complex has an essential role in spliceosomal snRNP biogenesis. *Cell*. 90:1023–1029.

Fyrberg, E.A., J.W. Mahaffey, B.J. Bond, and N. Davidson. 1983. Transcripts of the six *Drosophila* actin genes accumulate in a stage- and tissue-specific manner. *Cell*. 33:115–123.

Gabanella, F., C. Carissimi, A. Usiello, and L. Pellizzoni. 2005. The activity of the spinal muscular atrophy protein is regulated during development and cellular differentiation. *Hum. Mol. Genet.* 14:3629–3642.

Giesemann, T., S. Rathke-Hartlieb, M. Rothkegel, J.W. Bartsch, S. Buchmeier, B.M. Jockusch, and H. Jockusch. 1999. A role for polyproline motifs in the spinal muscular atrophy protein SMN. Profilins bind to and colocalize with smn in nuclear gems. *J. Biol. Chem.* 274:37908–37914.

Guettier-Sigrist, S., B. Hugel, G. Coupin, J.M. Freyssinet, P. Poindron, and J.M. Warter. 2002. Possible pathogenic role of muscle cell dysfunction in motor neuron death in spinal muscular atrophy. *Muscle Nerve*. 25:700–708.

Hauser, M.A., S.K. Horrigan, P. Salmikangas, U.M. Torian, K.D. Viles, R. Dancel, R.W. Tim, A. Taivainen, L. Bartoloni, J.M. Gilchrist, et al. 2000. Myotilin is mutated in limb girdle muscular dystrophy 1A. *Hum. Mol. Genet.* 9:2141–2147.

Hebbar, S., and J.J. Fernandes. 2004. Pruning of motor neuron branches establishes the DLM innervation pattern in *Drosophila*. *J. Neurobiol.* 60:499–516.

Ilangovan, R., W.L. Marshall, Y. Hua, and J. Zhou. 2003. Inhibition of apoptosis by Z-VAD-fmk in SMN-depleted S2 cells. *J. Biol. Chem.* 278:30993–30999.

Johansen, J., M.E. Halpern, and H. Keshishian. 1989. Axonal guidance and the development of muscle fiber-specific innervation in *Drosophila* embryos. *J. Neurosci.* 9:4318–4332.

Knight, P.J., and J.A. Trinick. 1982. Preparation of myofibrils. *Methods Enzymol.* 85:9–12.

Laing, N.G., and K.J. Nowak. 2005. When contractile proteins go bad: the sarcomere and skeletal muscle disease. *Bioessays*. 27:809–822.

Lefebvre, S., L. Burglen, S. Reboullet, O. Clermont, P. Burlet, L. Viollet, B. Benichou, C. Cruaud, P. Millasseau, M. Zeviani, et al. 1995. Identification and characterization of a spinal muscular atrophy-determining gene. *Cell*. 80:155–165.

Lorson, C.L., J. Strasswimmer, J.M. Yao, J.D. Baleja, E. Hahnen, B. Wirth, T. Le, A.H. Burghes, and E.J. Androphy. 1998. SMN oligomerization defect correlates with spinal muscular atrophy severity. *Nat. Genet.* 19:63–66.

McWhorter, M.L., U.R. Monani, A.H. Burghes, and C.E. Beattie. 2003. Knockdown of the survival motor neuron (Smn) protein in zebrafish causes defects in motor axon outgrowth and pathfinding. *J. Cell Biol.* 162:919–931.

Meister, G., D. Buhler, R. Pillai, F. Lottspeich, and U. Fischer. 2001. A multiprotein complex mediates the ATP-dependent assembly of spliceosomal U snRNPs. *Nat. Cell Biol.* 3:945–949.

Miguel-Aliaga, I., Y.B. Chan, K.E. Davies, and M. van den Heuvel. 2000. Disruption of SMN function by ectopic expression of the human SMN gene in *Drosophila*. *FEBS Lett.* 486:99–102.

Monani, U.R. 2005. Spinal muscular atrophy: a deficiency in a ubiquitous protein; a motor neuron-specific disease. *Neuron*. 48:885–896.

Moreira, E.S., T.J. Wiltshire, G. Faulkner, A. Nilforoushan, M. Vainzof, O.T. Suzuki, G. Valle, R. Reeves, M. Zatz, M.R. Passos-Bueno, and D.E. Jenne. 2000. Limb-girdle muscular dystrophy type 2G is caused by mutations in the gene encoding the sarcomeric protein telethonin. *Nat. Genet.* 24:163–166.

Muqit, M.M., J. Moss, C. Sewry, and R.J. Lane. 2004. Phenotypic variability in siblings with type III spinal muscular atrophy. *J. Neurol. Neurosurg. Psychiatry*. 75:1762–1764.

Narayanan, U., T. Achsel, R. Lührmann, and A.G. Matera. 2004. Coupled in vitro import of U snRNPs and SMN, the Spinal Muscular Atrophy protein. *Mol. Cell*. 16:223–234.

Nicole, S., B. Desforges, G. Millet, J. Lesbordes, C. Cifuentes-Diaz, D. Vertes, M.L. Cao, F. De Backer, L. Languille, N. Roblot, et al. 2003. Intact satellite cells lead to remarkable protection against Smn gene defect in differentiated skeletal muscle. *J. Cell Biol.* 161:571–582.

Nicole, S., C.C. Diaz, T. Frugier, and J. Melki. 2002. Spinal muscular atrophy: recent advances and future prospects. *Muscle Nerve*. 26:4–13.

Nongthomba, U., and N.B. Ramachandra. 1999. A direct screen identifies new flight muscle mutants on the *Drosophila* second chromosome. *Genetics*. 153:261–274.

Ogino, S., and R.B. Wilson. 2004. Spinal muscular atrophy: molecular genetics and diagnostics. *Expert Rev. Mol. Diagn.* 4:15–29.

Okamoto, H., Y. Hiromi, E. Ishikawa, T. Yamada, K. Isoda, H. Maekawa, and Y. Hotta. 1986. Molecular characterization of mutant actin genes which induce heat-shock proteins in *Drosophila* flight muscles. *EMBO J.* 5:589–596.

Otey, C.A., and O. Carpen. 2004. Alpha-actinin revisited: a fresh look at an old player. *Cell Motil. Cytoskeleton*. 58:104–111.

Patel, N.H. 1994. Imaging neuronal subsets and other cell types in whole-mount *Drosophila* embryos and larvae using antibody probes. *Methods Cell Biol.* 44:445–487.

Pellizzoni, L., J. Yong, and G. Dreyfuss. 2002. Essential role for the SMN complex in the specificity of snRNP assembly. *Science*. 298:1775–1779.

Rossoll, W., S. Jablonka, C. Andreassi, A.K. Kroning, K. Karle, U.R. Monani, and M. Sendtner. 2003. Smn, the spinal muscular atrophy-determining gene product, modulates axon growth and localization of beta-actin mRNA in growth cones of motoneurons. *J. Cell Biol.* 163:801–812.

Sarnat, H.B. 1992. Vimentin and desmin in maturing skeletal muscle and developmental myopathies. *Neurology*. 42:1616–1624.

Selcen, D., and A.G. Engel. 2003. Myofibrillar myopathy caused by novel dominant negative alpha B-crystallin mutations. *Ann. Neurol.* 54:804–810.

Shafey, D., P.D. Cote, and R. Kothary. 2005. Hypomorphic Smn knockdown C2C12 myoblasts reveal intrinsic defects in myoblast fusion and myotube morphology. *Exp. Cell Res.* 311:49–61.

Sharma, A., A. Lambrechts, T. Hao le, T.T. Le, C.A. Sewry, C. Ampe, A.H. Burghes, and G.E. Morris. 2005. A role for complexes of survival of motor neurons (SMN) protein with gemins and profilin in neurite-like cytoplasmic extensions of cultured nerve cells. *Exp Cell Res.* 309:185–197.

Shimizu, N., S. Kamel-Reid, and R. Zak. 1988. Expression of actin mRNAs in denervated chicken skeletal muscle. *Dev. Biol.* 128:435–440.

Shpargel, K.B., and A.G. Matera. 2005. Gemin proteins are required for efficient assembly of Sm-class ribonucleoproteins. *Proc. Natl. Acad. Sci. USA*. 102:17372–17377.

Szliwowski, H.B., and P. Drochmans. 1975. Ultrastructural aspects of muscle and nerve in Werdnig-Hoffmann disease. *Acta Neuropathol. (Berl.)*. 31:281–296.

Vajsar, J., T. Balslev, P.N. Ray, J. Siegel-Bartelt, and V. Jay. 1998. Congenital cytoplasmic body myopathy with survival motor neuron gene deletion or Werdnig-Hoffmann disease. *Neurology*. 53:873–875.

Wan, L., D.J. Battle, J. Yong, A.K. Gubitz, S.J. Kolb, J. Wang, and G. Dreyfuss. 2005. The survival of motor neurons protein determines the capacity for snRNP assembly: biochemical deficiency in spinal muscular atrophy. *Mol. Cell. Biol.* 25:5543–5551.

Winkler, C., C. Eggert, D. Gradl, G. Meister, M. Giegerich, D. Wedlich, B. Laggerbauer, and U. Fischer. 2005. Reduced U snRNP assembly causes motor axon degeneration in an animal model for spinal muscular atrophy. *Genes Dev.* 19:2320–2330.